Toward an estimation of the clarinet reed pulse from instrument performance

Tamara Smyth[a)]
School of Computing Science, Simon Fraser University, 250-13450 102nd Avenue, Surrey, British Columbia, V3T 0A3, Canada

Jonathan S. Abel
Department of Music, Center for Computer Research in Music and Acoustics (CCRMA), Stanford University, Stanford, California 94305-8180

(Received 22 June 2011; revised 1 March 2012; accepted 2 March 2012)

In this work, a technique is presented for estimating the *reed pulse* from the pressure signal recorded at the bell of a clarinet during performance. The reed pulse is a term given to the typically periodic sequence of bore input pressure pulses, a signal related to the volume flow through a vibrating reed by the characteristic impedance of the aperture to the bore. The problem is similar to extracting glottal pulse sequence from recorded speech; however, because the glottis and instrument reeds have very different masses and opening areas, the source-filter model used in speech processing is not applicable. Here, the reed instrument is modeled as a pressure-controlled valve coupled to a bi-directional waveguide, with the output pressure approximated as a linear time invariant transformation of the product of reed volume flow and the characteristic impedance of the bore. By noting that pressure waves will make two round trips from the mouthpiece to the bell and back for each reed pulse, yielding a distinct positive and negative lobe in the running autocorrelation period of the recorded signal, the round-trip attenuation experienced by pressure waves in the instrument is estimated and used to invert the implied waveguide, producing reed pulse estimates. © *2012 Acoustical Society of America*. [http://dx.doi.org/10.1121/1.3699211]

PACS number(s): 43.75.Zz, 43.75.Wx, 43.75.Ef, 43.60.Pt [TRM] Pages: 4799–4810

I. INTRODUCTION

It is common practice for contemporary musicians to explore a variety of playing techniques, often producing sounds that may be considered unusual and atypical of their instrument. Extended playing techniques are being increasingly employed by very accomplished musicians and, as in the case of reed-based wind instruments, require highly proficient and virtuosic control of vocal tract and embouchure to regulate airflow into the instrument.

Performers of acoustic instruments wishing to employ computer generated sound synthesis and effects to further augment their instrument's sonic palette must have some way to interface themselves with the computer so their musical intention may be transmitted through gesture, acquired and rendered as control data, and mapped to the input of a parametric algorithm. Expression, and the production of quality sound, is difficult on virtual instruments if the performer is not equipped with a device that is sufficiently responsive, ergonomic, and intuitive.

One approach to electronically augmenting an acoustic instrument is to obtain a player's control data by fitting sensors directly on the acoustic instrument. Though this approach can produce successful artistic results (see, e.g., Ref. 1), it can also yield a capricious and temperamental instrument, with its stability being hampered by unwieldy wires and sensors that also crowd the instrument's performance space and sometimes fail when coming into contact with the musician. Unfortunately, many such tools and inventions quickly fall from use before they can be sufficiently developed and practiced, and their potential as musical instruments is often only demonstrated by the inventor.

Another way for a musician to gain access to interactive sound effects/synthesis algorithms is to replace their instrument entirely with a commercially available controller—an increasingly popular choice with the availability of wind controllers offering an alternative to the keyboard interface and allowing wind players use of the fingering techniques with which they are more familiar. Yet commercial controllers remain committed to, and thus employ, the Musical Instrument Digital Interface (MIDI) standard, a low-resolution protocol that is not always sufficient for expressing desired nuances [though this problem is gradually being corrected with the widening use of Open Sound Control (OSC)].[27] Additionally, and perhaps even more significantly, there is a limit to the sensitivity of these devices, as well as to which physical parameters can be measured—particularly at the level of embouchure, making it difficult to capture fine gestural changes that distinguish a player's individual articulatory style. One final consideration is that a controller removes the player from the feedback loop connecting control with the instrument's produced sound, creating further challenges for the player. Musicians are generally more virtuosic on acoustic instruments than computer input devices, likely in part because of the difference in time devoted to

a)Author to whom correspondence should be addressed. Electronic mail: tamaras@cs.sfu.ca

practice, but also because of the difference in haptic, auditory, and acoustic feedback.[2] It is well known, for example, that buzzing one's lips at the end of a cylindrical tube is a rather different experience than at the mouthpiece of a trumpet, with the bore and bell serving to shift resonant peaks in the instrument's frequency response.

As a third alternative for computer music interaction, therefore, researchers are increasingly addressing the problem of deriving a model's control parameters from recordings of an acoustic system's produced sound, that is, *the inverse problem*.[3–7] Inverting models by calibrating to recorded data can validate a physics-based model,[8,9] improve playability of its often extremely rich parameter space,[10] or allow for use of estimated parameter values for control of another processing algorithm.

For wind instruments, one of the primary ways in which a performer controls sound production, aside from changing pitch using instrument tone holes/keys, is by changing the airflow into the bore through alterations of blowing pressure and embouchure. For example, *side tonguing* creates a muffled effect by using the tongue to reduce the amount of airflow into the mouthpiece; *flutter tonguing* is a technique whereby the tongue rapidly opens and closes the airflow into the mouthpiece; *pitch bend* is a technique whereby the player changes the embouchure to sharpen or flatten the pitch; *subtones* are created by using the least possible amount of air to sound a note; and *vocalizing* is a technique whereby the player speaks or sings into the horn, placing the vibrating vocal folds in series with the saxophone reed, creating an amplitude modulation effect that produces a "split" tone.

Postulating that if a playing technique allows for a perceptible difference in the produced sound, the sound signal must also in turn hold information about the employed playing gesture, the ultimate aim in this research is to estimate aspects of the clarinetist's control input using only a microphone that passively records the acoustic pressure signal produced at the bell of the instrument, and requires no other inhibiting or intervening hardware.

The research herein, therefore, focuses on an important initial step toward this goal, and presents a technique for estimating the signal generated by the reed, from the signal measured at the bell, using acoustic measurement, post-processing, and inverse filtering. The estimated pressure signal is related to volume flow U by the bore's characteristic impedance Z_0, and is henceforth referred to as the *reed pulse* or *reed pulse sequence,* a term intended as a nod to the similar problem of estimating the glottal pulse in speech processing, and also to illustrate its expected pulse-train-like nature, as established in Sec. IV. As the reed pulse holds information related to airflow into the bore, embouchure, and high-level standard and extended playing techniques, it is expected that its estimation is a prerequisite to further extracting playing parameters that are more subtle than simply the pitch (tone hole configuration) of the instrument. Once the reed pulse is isolated, parameter values may be gleaned by observing the characteristic behaviors of the signal (such as contours, closure rates, value-crossings, etc.) or by calibrating to the output of a physical model of a reed (such as the one described in Sec. IV), allowing for estimation of physical playing parameters such as blowing pressure or the reed tension/resonance.

As mentioned earlier, the problem of estimating the reed pulse is similar to that of estimating a glottal pulse sequence from recorded speech. This is commonly done via mel-frequency cepstral coefficients (MFCCs) or linear predictive coding (LPC).[11] However, Lu and Smith presented a method where the formant filter and the glottal source are separately estimated via complex optimization.[12] As many wind instrument reeds have a much smaller mass and opening than those of the vocal folds (and this is indeed the case for the clarinet), they are consequently more effected by the internal state of the instrument, and generate a more significant reflection. As a result, the source-filter model used in speech processing is not expected to be valid here.

An example of recovering the parametric inputs of a trumpet physical model is described in Ref. 13. Their method derives an inverse filter using an anechoic measurement of the instrument's acoustic reflection function, with the inverse filter being applied to the recorded signal after adding a physical constraint to address an *ill-posed* problem. The assumption that the trumpet bore behaves as a one-dimensional waveguide with a pure delay that can be changed with pitch justifies their use of off-line measurements. This assumption, however, cannot be applied to the clarinet or any instrument having tone holes and for which the round-trip propagation will vary with a change of fingering. Changing the tone hole configuration will change the characteristic impedance along the bore, introducing a reflection and transmission at each open tone hole and thus a more significant change in the instrument's transfer function than simply the length of the propagation delay.

Sterling *et al.*[14] attempt to extract clarinet control parameters, but state they could not invert their clarinet instrument transfer function. Unable to isolate the reed pulse, they used the amplitude envelope of the recorded sound to roughly estimate blowing pressure. In van Walstijn and de Sanctis[15] a procedure is described for providing separate characterizations of the resonator and the driving signal for wind instruments. The solution focuses on separating traveling pressure waves, done by taking measurements at different positions along the instrument bore to obtain the reflection function at the open/bell end. Though the method produces good and important results, they are based on off-line measurements that require placing microphones inside their acoustic tube—more difficult when measuring an actual performing instrument to which you cannot make permanent modifications.

The work presented here further develops that in Ref. 16, which presents an expression for the transfer function from reed pulse to the sound pressure produced by a clarinet at the bell, as well as an expression for the inverse filter, given in terms of the instrument bell transmission, reflection, and propagation losses. The problem exposed in Ref. 16 is that the reed instrument transfer function is comprised of unknown waveguide elements (propagation losses, as well as reflection and transmission at the boundaries and any open tone holes) that would be needed before completing the inverse filter. Since most of these elements are expected to

change during performance, solely using off-line measurements would be insufficient for ultimately estimating the reed pulse from the instrument's produced sound. The work here improves upon the method reported in Ref. 16 for estimating round-trip propagation losses from the sound recorded at the bell, incorporates measurement of the bell's transmission function as well as a reed model to obtain a target for validating the closed-hole case, and presents results of inverse filtering that very closely match the desired target.

In Sec. II, the classic waveguide model of the clarinet, presented along with its waveguide filter elements, is used to follow the behavior of bore pressure in response to an input pressure pulse, as well as to introduce the periodic structure of the clarinet signal that forms the basis for estimating the reed pulse. In Sec. III, the reed-clarinet transfer function is developed from the input reed pulse X to the instrument's produced sound Y_L, establishing the inverse filter needed for estimating the reed pulse sequence. Unknown filter elements that comprise the inverse filter are obtained from measurement in Sec. IV for the special case of the clarinet's lowest note, establishing target behavior for subsequent evaluation for this particular case. Finally, in Sec. V, a more general technique is presented for estimating the reed pulse in the presence of *any* fingering/tone hole configuration. A filter corresponding to the round-trip instrument losses is estimated from the pressure signal at the bell and compared to the same filter constructed from measured waveguide elements. The validation of the closed-hole case, the case for which there is a target created using measured bell reflection/transmission functions, provides confidence that the method may be used for any tone hole configuration (since the estimation method makes no assumption of tone holes being closed).

II. CLARINET INSTRUMENT MODEL

Blowing into the mouthpiece of a reed instrument allows the player to control the reed's oscillation by creating a pressure difference across its surface. When the reed oscillates, it creates an alternating opening and closure to the bore, allowing airflow entry during the open phase and cutting it off during the closed phase. As shown in Sec. IV B, which describes a simple quasi-static clarinet reed model for further illustration, the effect is a periodic train of pressure pulses, the *reed pulse sequence,* into the bore. The oscillation of the reed, and thus the periodicity of the reed pulse, is also dependent on the pressure traveling to and fro along the length of the bore, a pressure which is subject to frequency-dependent losses according to the bore's length, size, shape, and termination.

It is well known that wave propagation in wind instrument bores may be approximated using the one-dimensional waveguide model structure shown in Fig. 1, with a bi-directional delay line of length M samples accounting for the acoustic propagation delay in the cylindrical and/or conical tube sections of a given length, and filter elements $\lambda(z)$, $R_M(z)$, $R_B(z)$, and $T_B(z)$, accounting for the propagation loss, reflection at the mouthpiece, and open-end reflection and transmission occurring at the bell, respectively. For this model to be valid for instruments

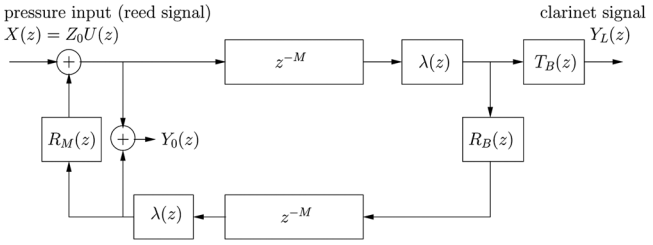

FIG. 1. Waveguide model of a clarinet bore and bell, with commuted propagation (wall) loss filters $\lambda(z)$ at upper and lower delay line observation points, open-end reflection and transmission filters $R_B(z)$ and $T_B(z)$, respectively, having acoustic properties of the bell, and a reflection filter at the position of the reed/mouthpiece $R_M(z)$. The pressure input into the system (the driving signal or *reed signal*) is the product of the volume flow $U(z)$ and the characteristic impedance Z_0. The waveguide is tapped at two positions corresponding to the mouthpiece and outside the bell, producing pressure outputs $Y_0(z)$ and $Y_L(z)$, respectively.

having tone holes (with open states creating reflection and transmission characteristics that may be lumped with that of the bell), all elements may contain delays, poles, or "long-memory" information on the acoustics of the non-cylindrical/non-conical bell section.[17–19]

In developing a strategy for extracting the reed pulse $x(t)$ from the instrument's produced sound $y_L(t)$ (where lowercase variables are used in the time-domain representation), it is instructive to observe how bore pressure behaves in response to input pressure by following the classic waveguide structure shown in Fig. 1. For a woodwind such as a clarinet, the initial position of the reed is open. Introducing mouth pressure creates a volume flow through the reed channel after which the reed closes (though not necessarily completely), resulting in a volume flow *pulse*. The product of the volume flow U and the characteristic impedance of the bore Z_0 creates a positive input pressure, or reed pulse $x(t)$ to the bore, which travels toward the bell along the bore length (creating a propagation delay of M samples) while being subjected to various propagation losses $\lambda(z)$, including viscous drag along the bore walls. Once the pressure reaches the bell (or an open tone hole), a part is inverted with transfer function $R_B(z)$ and sent propagating back along the bore to the mouthpiece, and a part is transmitted out the bell with transfer function $T_B(z)$. The reflected pressure is inverted, creating a negative pressure at the mouthpiece and further closing the reed. The negative pressure is reflected off the reed with transfer function $R_M(z)$ (an assumed uninverting and predominantly closed reflection) and is returned down the bore to the bell, again being subjected to further propagation and reflection loss. The now positive pressure at the mouthpiece $y_0(t)$ is sufficient to open the reed and allow for another reed pulse. The result is that the bore pressure will make two round trips from the mouthpiece to the bell and back for each reed pulse, with the first being positive, and the second being negative. In the presence of a periodic reed pulse sequence, therefore, the bore pressure $y_0(t)$ will also be periodic—with the same period but with two distinct halves; one where the pressure pulse is positive, and one where it is negative (illustrated in Fig. 2, and made lossless for improved visibility). As the periodicity and period structure of the signal measured at the bell $y_L(t)$ is expected to have a similar structure as the pressure at the mouthpiece $y_0(t)$, the recorded signal $y_L(t)$ will also display two distinct

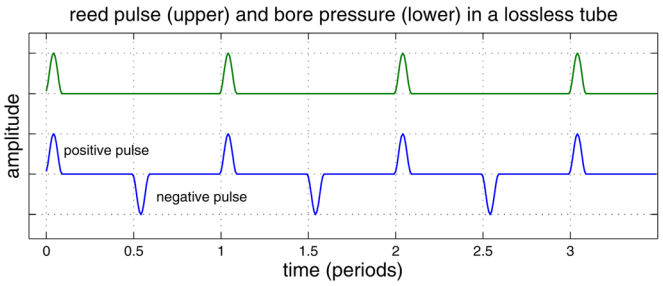

FIG. 2. (Color online) Bore pressure at the mouthpiece $y_0(t)$ (lower) will make two round trips from the mouthpiece to the bell and back for each input reed pulse $x(t)$ (upper). Given a periodic volume flow $U(t)$, and thus a periodic reed pulse $x(t)$, the bore pressure $y_0(t)$ will also be periodic with the same period, but will have two distinct halves to one reed pulse period—one where the pressure pulse is positive and one where it is negative. No losses are considered to better illustrate this fundamental concept.

halves to the period initiated by the reed pulse, though with a delay corresponding to the time required to travel the length of the bore and bell. This periodic structure, with the period having two distinct halves—one where the pressure pulse is positive and one where it is negative—provides the basis for estimating the reed pulse signal $x(t)$ given $y_L(t)$.

III. OBTAINING VOLUME FLOW BY INVERSE FILTERING

Ignoring the time-varying component in the reed/mouthpiece reflection, the clarinet response Y_L to input pressure $X = Z_0 U$ may be seen as a train wave, a succession of waves spaced at regular intervals, leading to a geometric series that may be expressed in the z domain as

$$\begin{aligned} Y_L(z) &= z^{-M}\lambda(z)T_B(z)[1 + z^{-2M}\lambda^2(z)R_M(z)R_B(z) \\ &\quad + z^{-4M}\lambda^4(z)R_M^2(z)R_B^2(z) + \cdots]X(z) \\ &= \frac{z^{-M}\lambda(z)T_B(z)}{1 - z^{-2M}\lambda^2(z)R_M(z)R_B(z)}X(z) \\ &= H(z)X(z), \end{aligned} \tag{1}$$

where M is the acoustic propagation time, in samples, required to travel the length of the instrument bore, and $H(z)$ is the clarinet reed pulse transfer function.

The reed pulse sequence $X(z)$ may then be obtained by inverse filtering, that is,

$$\begin{aligned} X(z) &= Y_L(z)/H(z) \\ &= \frac{1 - z^{-2M}\lambda^2(z)R_M(z)R_B(z)}{z^{-M}\lambda(z)T_B(z)}Y_L(z) \\ &= G(z)Y_L(z), \end{aligned} \tag{2}$$

where the inverse filter is given by

$$G(z) = \frac{1 - z^{-2M}\lambda^2(z)R_M(z)R_B(z)}{z^{-M}\lambda(z)T_B(z)}. \tag{3}$$

The inverse filter, therefore, has several unknowns: The bell reflection and transmission filters $R_B(z)$ and $T_B(z)$, respectively, the reed/mouthpiece reflection $R_M(z)$, and the propagation losses $\lambda(z)$ along the bore. Obtaining accurate responses for these waveguide filter elements is not necessarily straightforward, as all are expected to change during performance with an oscillating reed creating a time-varying component in the mouthpiece, as well as applied fingerings, opening and closing tone holes, resulting in radiation loss and scattering along the instrument bore, and thus the need to redefine $R_B(z)$ and $T_B(z)$ within the context of the waveguide structure seen in Fig. 1.

In Sec. IV, the model in Fig. 1, and corresponding inverse filter $G(z)$ given by Eq. (3), are constructed for the closed-hole case, since this is the case for which the bore may be approximated as a cylinder (neglecting chimneys), which is well described theoretically, and the bell reflection and transmission functions $R_B(z)$ and $T_B(z)$ may be accurately estimated using the measurement technique described in Sec. IV A, adapted from Ref. 20. Having the complete instrument model for the closed-hole case allows for coupling to a dynamic reed simulation (described in Sec. IV B), which provides a theoretical reed pulse and an expected "ideal" signal behavior to which estimations may be compared. The corresponding inverse filter $G(z)$ for the closed-hole case allows production of a "less ideal," but closer to actual, reed pulse signal, estimated from the pressure signal recorded at the bell of a clarinet playing its lowest note (as described in Sec. IV C). This provides a target case for validating the estimation technique described in Sec. V, which is applicable to any tone hole configuration and makes no assumption that the tone holes are closed.

IV. TARGET REED PULSE FOR THE CLOSED-HOLE CASE

To obtain a target behavior of the reed pulse signal, the unknowns comprising the model in Fig. 1 and the inverse filter $G(z)$ [Eq. (3)] are completed using both theory and measurement for the case where all tone holes are closed. Preliminary results are then obtained by directly applying the inverse filter (3) to the lowest note played on a B-flat clarinet, played with all the tone holes closed, and recorded outside the bell. Because this instrument configuration has no open tone holes causing loss and scattering along the bore length, it may be reasonably approximated as a cylinder (omitting chimneys) and modeled using the waveguide structure in Fig. 1, with wall losses well described theoretically, reed mouthpiece reflection R_M approximated, and bell reflection and transmission function, R_B and T_B, respectively, obtained using the measurement technique described herein.

A. Obtaining bell reflection and transmission functions

Though the inverse filter (3) and instrument model described by Fig. 1 are still valid for instrument configurations having open tone holes, the acoustic behavior resulting from tone hole radiation and scattering is lumped into $R_B(z)$ and $T_B(z)$, and thus these elements, within the context of the waveguide model in Fig. 1, would hold more information than solely the acoustic behavior of the bell. For this reason, the method described herein for obtaining estimations of bell

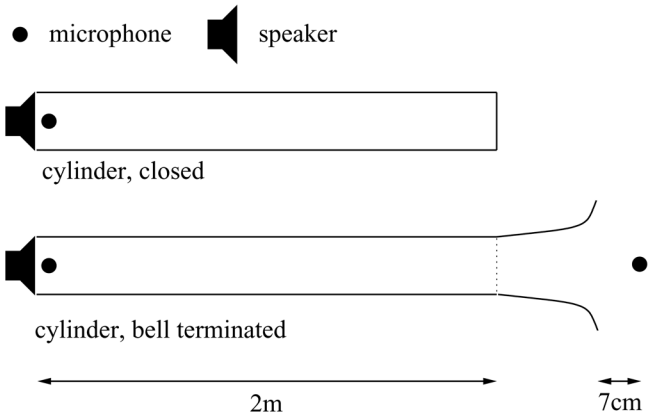

FIG. 3. The measurement system, showing a 2 m tube terminated at one end with a speaker, and at the other (1) closed (top), and (2) with a clarinet bell (bottom). The speaker provides a driving signal, while a co-located microphone, as well as one placed 7 cm outside the bell, records the response.

reflection and transmission from measurement, $\hat{R}_B(\omega)$ and $\hat{T}_B(\omega)$, respectively, is only applicable to the model of the clarinet having all tone holes closed. (Note: This method would, however, likely work well for a trombone, with the bore being well approximated as a cylinder of varying length, and the bell also being easily removed and measured.)

The measurement and post-processing technique used to estimate the bell reflection and transmission filters expands upon a technique fully described in Ref. 20 for obtaining waveguide elements from several measurements of a system's impulse response. A measurement is taken of a system having incrementally varying termination/boundary conditions. The post-signal processing begins by expressing each of the echos seen in the impulse response in terms of composite waveguide filter elements. Further manipulation of these expressions allows for isolation and estimation of filters seen in Fig. 4, adapted from Fig. 1 but showing elements related to the measurement system that must also be taken into account when estimating elements comprising the inverse filter in Eq. (3). The technique described here is also used in Ref. 19 for obtaining bell reflection and transmission functions to improve synthesis accuracy in a waveguide synthesis model of a trombone.

As described in Refs. 19 and 20, measurements are taken of a 2-m-long PVC pipe, terminated at one end with a speaker [CUI Inc (Tualatin, OR) CMS020KLX], and at the opposite end with (1) a piece of flat plastic assumed to be perfectly reflective and (2) a clarinet bell. A microphone capsule (omnidirectional electret condenser microphone cartridge, JL-061C) is embedded in the pipe wall as close to the speaker as possible, with another of the same model placed within 7 cm of, and on axis with, the tube/bell. The measurement system is illustrated in Fig. 3, and may be modeled as per Fig. 4, adapted from Fig. 1 to include filter elements related to the measurement system.

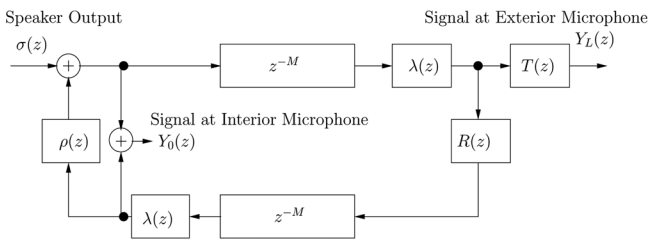

FIG. 4. Waveguide model of a cylindrical tube adapted from Fig. 1, with microphone capturing signal response $Y_0(z)$ at the tube base, and a co-located speaker having a transmission function of $\sigma(z)$ and a reflection function of $\rho(z)$. At the opposite end there are two possible terminating conditions: (1) $R(z) = 1$ and $T(z) = 0$ for a closed tube, and (2) $R(z) = R_B(z)$ and $T(z) = T_B(z)$ for the appended clarinet bell.

For both the closed and bell-terminated systems seen in Fig. 3, a test signal, a logarithmic swept sinusoid of sufficient length (20 s) to ensure a sufficiently large signal-to-noise ratio (SNR),[21] is used to drive the speaker, with the response, $y_0(t)$ and $y_L(t)$, being recorded at the interior and exterior microphones, respectively. The peak level for $y_0(t)$ measured approximately 90 dB above the noise floor standard deviation, whereas the SNR for $y_L(t)$ was approximately 70 dB, both using a 20-s-long test signal. Note: Though no signal is expected at the outside microphone for the closed tube, the recorded response may be used to verify there is little or no leakage from the closed end.

As described by Ref. 21, the signals recorded at the two microphones, $y_0(t)$ and $y_L(t)$ are linearly deconvolved to separate non-linear harmonic distortion (caused by the speaker) from the desired linear impulse response. Following this post-processing, and assuming both a microphone magnitude response that is flat in the band of interest and no prior circulating energy in the tube, the first three arrivals for the closed tube L_n, windowed from the impulse response seen in Fig. 5 (top), are given by

$$L_1(\omega) = \sigma(\omega), \tag{4}$$

$$L_2(\omega) = \sigma(\omega)\lambda^2(\omega)(1 + \rho(\omega)), \tag{5}$$

$$L_3(\omega) = \sigma(\omega)\lambda^4(\omega)\rho(\omega)(1 + \rho(\omega)), \tag{6}$$

where $\sigma(\omega)$ is the speaker transmission function (the frequency response of the speaker), $\rho(\omega)$ is the frequency response of the function describing the reflection off the speaker, and $\lambda^2(\omega)$ is the frequency response of the round-trip propagation losses for a cylinder. The function of ω is used in lieu of z to distinguish measurement from the theoretical representation used in Fig. 4.

Changing the rigid termination at the end opposite the speaker by appending a clarinet bell produces the system in Fig. 3 (lower), and introduces the bell reflection in the response arrivals at both microphones. The arrival responses $B_{0,n}$ for the bell-terminated tube at the microphone positioned next to the speaker are windowed from the impulse response seen in Fig. 5 (middle), the first three of which are given by

$$B_{0,1} = \sigma(\omega), \tag{7}$$

$$B_{0,2} = \sigma(\omega)\lambda^2(\omega)R_B(\omega)(1 + \rho(\omega)), \tag{8}$$

$$B_{0,3} = \sigma(\omega)\lambda^4(\omega)\rho(\omega)R_B^2(\omega)(1 + \rho(\omega)). \tag{9}$$

The bell reflection may be estimated by taking the ratio of the second arrival spectra from the bell-terminated and closed tubes:

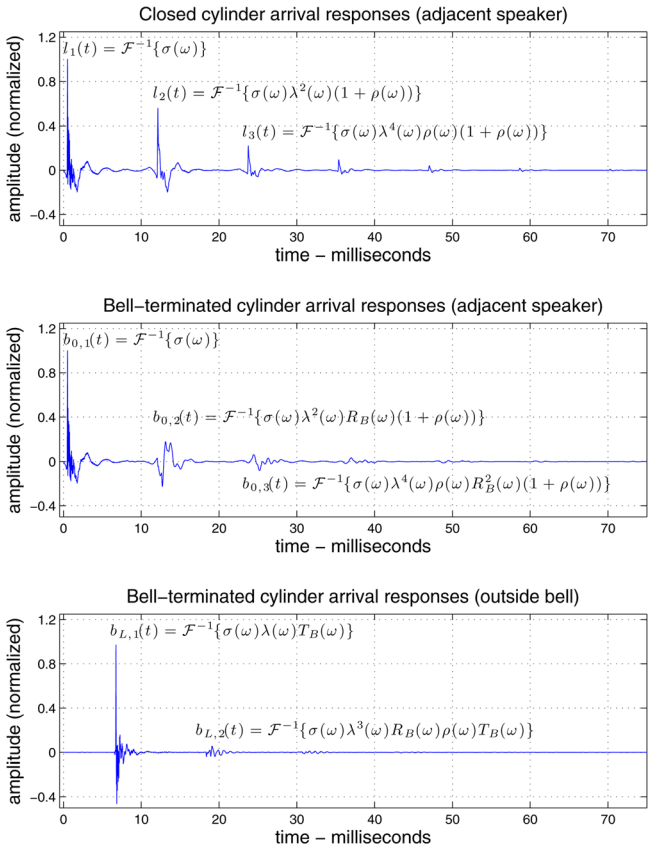

FIG. 5. (Color online) Measured impulse responses for the closed cylinder (top), bell-terminated cylinder (middle), and bell-terminated cylinder outside the bell (bottom), showing individual arrivals as their inverse transforms.

$$\hat{R}_B(\omega) = \frac{B_{0,2}(\omega)}{L_2(\omega)} = \frac{\sigma(\omega)\lambda^2(\omega)R_B(\omega)(1+\rho(\omega))}{\sigma(\omega)\lambda^2(\omega)(1+\rho(\omega))}, \quad (10)$$

with the resulting frequency response magnitude being plotted in Fig. 6 (upper) and showing an expected low-pass characteristic.

The arrival responses $B_{L,n}$ for the bell-terminated tube at the microphone positioned 7 cm outside, and on axis with, the bell, are windowed from the impulse response seen in Fig. 5 (bottom), the first two of which are given by

$$B_{L,1} = \sigma(\omega)\lambda(\omega)T_B(\omega), \quad (11)$$

$$B_{L,2} = \sigma(\omega)\lambda^3(\omega)R_B(\omega)\rho(\omega)T_B(\omega). \quad (12)$$

The bell transmission may be estimated from the first arrival $B_{L,1}$ by dividing Eq. (11) by the product of the speaker transmission (4) and the cylindrical propagation losses $\lambda(\omega)$, yielding

$$\hat{T}_B(\omega) = \frac{B_{L,1}(\omega)}{L_1(\omega)\lambda(\omega)} = \frac{\sigma(\omega)\lambda(\omega)T_B(\omega)}{\sigma(\omega)\lambda(\omega)}, \quad (13)$$

where the propagation losses $\lambda(\omega)$ may be obtained either theoretically or using an additional measurement of an open cylinder as described in Ref. 20. The resulting bell transmission frequency response magnitude is plotted in Fig. 6 (lower), showing an expected high-pass characteristic.

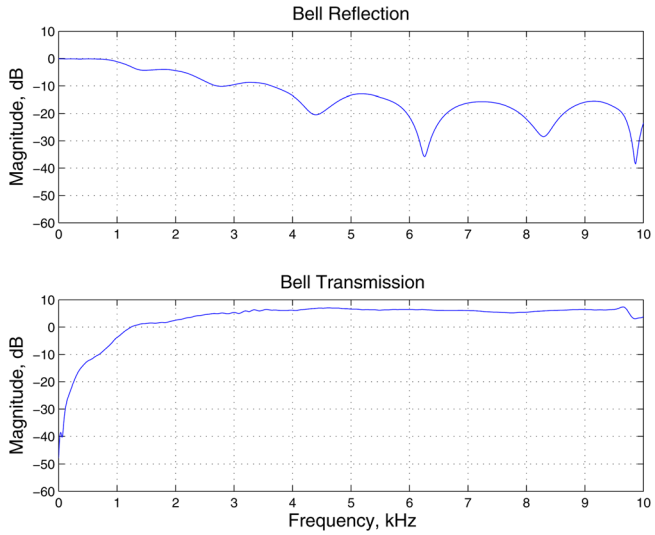

FIG. 6. (Color online) Bell reflection and transmission filter magnitudes. As expected, the former shows a low-pass characteristic, while the latter shows a high-pass characteristic.

B. A model of the reed pulse

Before estimating the reed pulse X from the clarinet signal Y_L, it is useful to gain an understanding of what type of signal is expected, and how it might change under different playing conditions. As previously stated, it is expected that the reed pulse signal behaves like a pulse train, with pulses typically followed by periods of reed closure if the player blows sufficiently hard that the reed beats against the lay of the mouthpiece. This assumption is illustrated by a simple quasi-static model of volume flow U through the reed channel. Though this model is chosen here for illustration clarity, a dynamic model may be preferable for sound synthesis.[22]

In the presence of an applied mouth (blowing) pressure, a pressure difference Δp is created across the reed between the valve's upstream (mouth) and downstream (bore) pressures, setting the reed into motion with a displacement that may be approximated by

$$x_d(t) = \frac{\Delta p(t)}{\kappa}, \quad (14)$$

where κ describes the reed stiffness (in Pa/m). Note that Eq. (14) may be derived from the familiar second-order differential equation for a simple harmonic oscillator by setting the derivatives to zero, rendering the reed effectively massless, and leaving κ as the only reactive element.[23] As the reed vibrates, the displacement toward, and away, from the lay of the mouthpiece creates a variable opening to the bore through which volume flow may pass at a steady-state rate approximated by the stationary Bernoulli equation,

$$U(t) = A(t)\sqrt{\frac{2\Delta p(t)}{\rho}}, \quad (15)$$

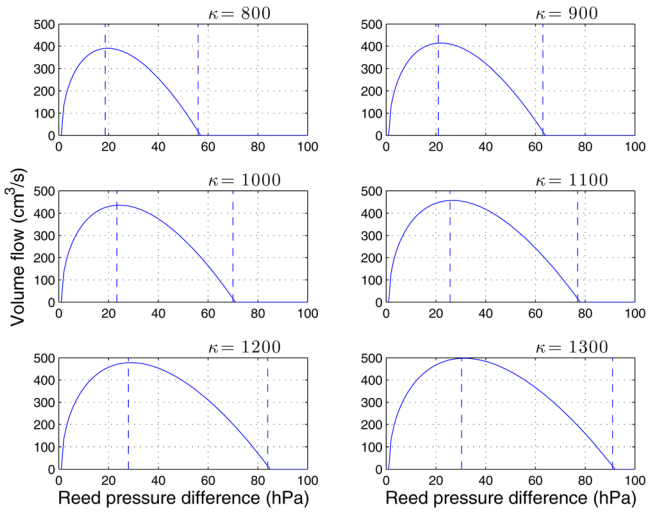

FIG. 7. (Color online) The volume flow U as a function of change in pressure across the reed Δp produces a pulse-like shape followed by a horizontal line above the maximum pressure difference $\Delta p_{\max}$. The maximum flow $U_{\max}$ is reached at $\Delta p_{\max max}/3$, and corresponds to the threshold of oscillation while $\Delta p_{\max}$ corresponds to zero flow and a closed reed. Notice how the shape of the volume flow pulse, defined by the maximum volume flow $U_{\max}$ and the maximum pressure difference $\Delta p_{\max}$, changes with a change in reed stiffness, a parameter that typically corresponds to the player's embouchure, suggesting the flow signal may be useful in extracting playing parameters related to timbral control.

where ρ is air density, and $A(t)$ is the cross sectional area, given by the product of the jet's (valve channel's) width w and height,

$$A(t) = w(H_0 - x_d(t)), \tag{16}$$

where H_0 is the equilibrium opening, the opening of the valve channel in the absence of flow. As seen in Fig. 7, when plotted as a function of pressure difference, the volume flow produces a pulse-like shape during the reed's open state, reaching a maximum volume flow of

$$U_{\max} = wH_0 \frac{2}{3}\sqrt{\frac{2\Delta_p \max}{3\rho}}, \tag{17}$$

at $\Delta p_{\max}/3$, followed by zero volume flow at the maximum pressure difference,

$$\Delta p_{\max} = \kappa H_0, \tag{18}$$

above which the reed is closed.

When this reed model, known as the quasi-static reed model,[22–25] is coupled to the waveguide model of the instrument bore, the synthesized clarinet output, obtained using the closed-hole case of either, either Eq. (1) or the time-domain waveguide model illustrated in Fig. 1, completed with bell filter elements estimated as in Sec. IV A, results in the produced sound and corresponding reed pulse sequence seen in Fig. 8. Figure 8 shows the model at various stages of the note, the attack, the steady state, and the note release, with the reed pulse characteristic being most prominent during the non-transient sustained component of the note.

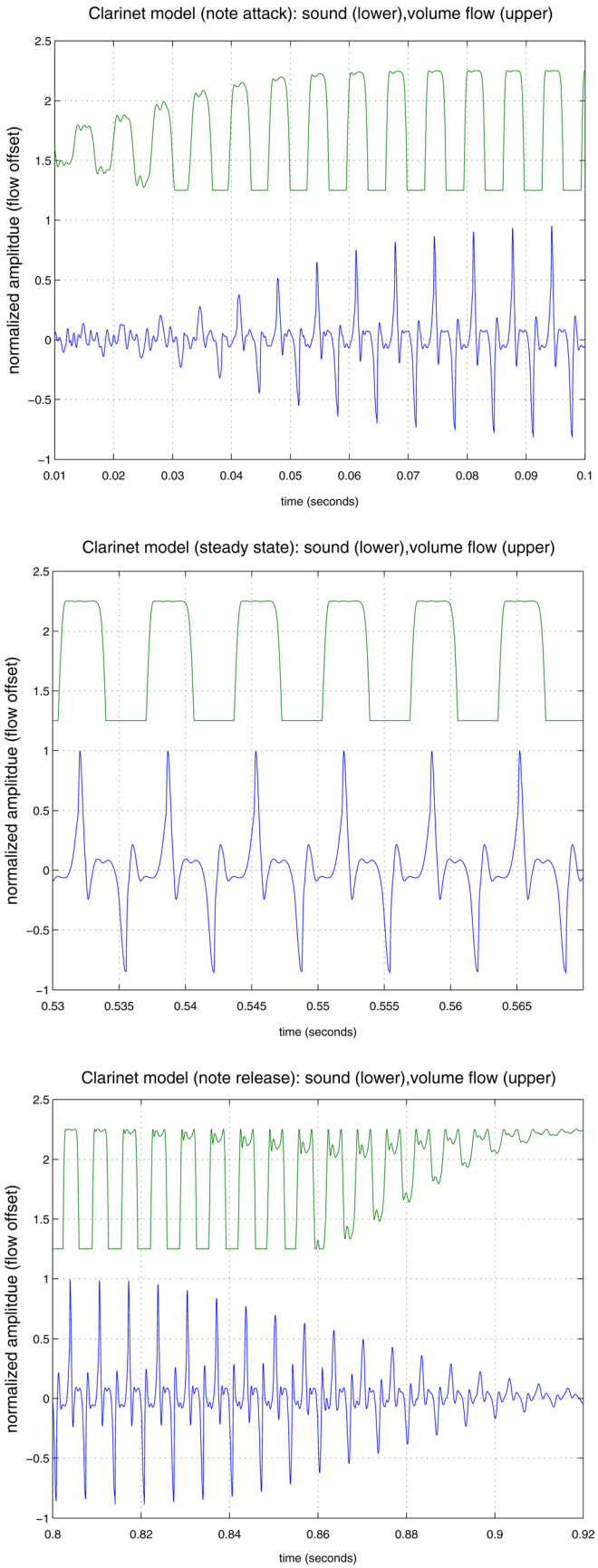

FIG. 8. (Color online) Outputs of the clarinet reed coupled to a waveguide model shown at various stages of a note: At the note onset (attack), the note sustain (steady state) and the note release (decay). Both volume flow and sound transmitted at the bell are shown, so that the relationship between the flow pulse and the clarinet signal may be observed.

C. Preliminary estimation results

Preliminary results of estimating the reed pulse from an actual recording, shown in Fig. 9, are obtained by applying the inverse filter (3) to the special case of the lowest note played on a clarinet having the same bell, and using the same recording microphone, in the same position, as in the measurement setup of Sec. IV A. With all the tone holes on the clarinet closed, it is assumed there is no radiation loss or scattering along the clarinet bore (ignoring the tone hole chimneys), justifying the use of a theoretically modeled cylindrical wall loss filter for bore propagation loss $\lambda(z)$, shown to be accurate when designed according to a cylinder's length and radius.[26] This instrument configuration is expected to most closely match the model given by Eq. (1) when completed with the measured bell reflection (10) and transmission (13) function obtained as per Sec. IV A, and thus likely yielding the most accurate estimation of the reed pulse sequence possible with known waveguide elements.

It should be noted, however, that the approximations made in constructing the instrument model and its inverse (3), in particular setting $R_M(z) = 0.9$, omitting the effects of the mouthpiece, and, likely less significantly, omitting the effects of the tone hole chimneys, will only allow for estimation of an *approximate* target reed pulse, its accuracy being dependent on the accuracy of the approximation(s). The more general method presented in Sec. V (not limited to the closed-hole case) that estimates the *lumped* round-trip losses of the instrument (i.e., it does not rely on having values for individual waveguide elements) makes no approximations of waveguide elements, and may thus yield a more accurate estimation of the reed pulse than the preliminary target presented here—even for the closed-hole case. That is, it is not expected that the estimated reed pulse signals will be exact for each technique, but that they will be very similar and exhibit the behavior expected of a reed pulse sequence (as described in Sec. IV B).

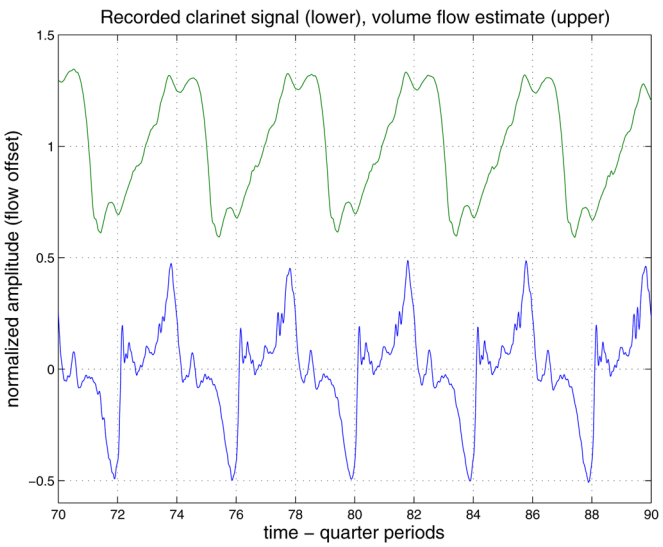

FIG. 9. (Color online) A recording of the lowest note on a clarinet played with all tone holes closed (lower) is shown with estimated volume flow pulses (upper) obtained by directly applying inverse filter (3), with waveguide elements obtained theoretically and by applying the measurement technique described in Sec. IV A.

V. ESTIMATING THE REED PULSE FOR THE GENERAL CASE

The preliminary results obtained in Sec. IV C for a recording of the clarinet's lowest note display behavior that is expected of a reed pulse signal: The signal is periodic with the same period as the recorded signal, with each reed pulse in the sequence being followed by a segment of partial or complete reed closure. The corresponding period of the recorded pressure signal displays the expected two distinct halves, one where the pressure pulse is positive, followed by one where it is negative, with the overall period having a phase relationship to the volume flow pulses that closely matches that seen in the model's steady-state output, shown in Fig. 8 (middle).

As previously mentioned, the waveguide elements comprising the inverse filter in Eq. (3) are expected to change during performance. Opening and closing tone holes will invalidate estimated bell reflection and transmission filters, $\hat{R}_B(\omega)$ and $\hat{T}_B(\omega)$, obtained using the measurement and post-processing technique described in Sec. IV A, within the assumed waveguide structure seen in Fig. 1. In addition, it is possible that propagation losses are no longer as accurately described theoretically, though this is of less concern as these losses are relatively small. More significantly, as mentioned earlier, the preliminary results do not account for the effects of the mouthpiece, a model component that is more difficult to model and/or measure. Because of the time-varying nature of the problem in completing the inverse filter (3) for the more general case (for an instrument where each tone hole may be either open or closed), a technique is needed for *dynamically* estimating filter elements, either lumped or individually, during instrument performance. So as not to impact the player or encroach on their playing space, it is most preferable to estimate these losses directly from the signal recorded outside the clarinet bell.

A. Inferring round-trip propagation losses

Assume that for over a short period of time the reed pulses do not change substantially, that is, they are periodic. In the presence of a periodic output $y_L(t)$, the copies of the reed instrument response to prior reed pulses are aligned in time. This can be seen in Fig. 10, where instrument impulse responses are incrementally time shifted to the left by one period to show that a given period 4τ, the time taken for two round trips from the mouthpiece to the bell and back again, will be in phase with previous periods, and that the positive and negative pulses making up the period will align in time.

Denoting the losses due to one round-trip propagation from the mouthpiece to the bell and back again by

$$\eta(z) = \lambda^2(z) R_B(z) R_M(z), \tag{19}$$

the reed instrument signal transform can be written as

$$Y_L(z) = z^{-M} \lambda(z) T(z) \left[\frac{1 + z^{-2M} \eta(z)}{1 - z^{-4M} \eta^2(z)} \right] X(z), \tag{20}$$

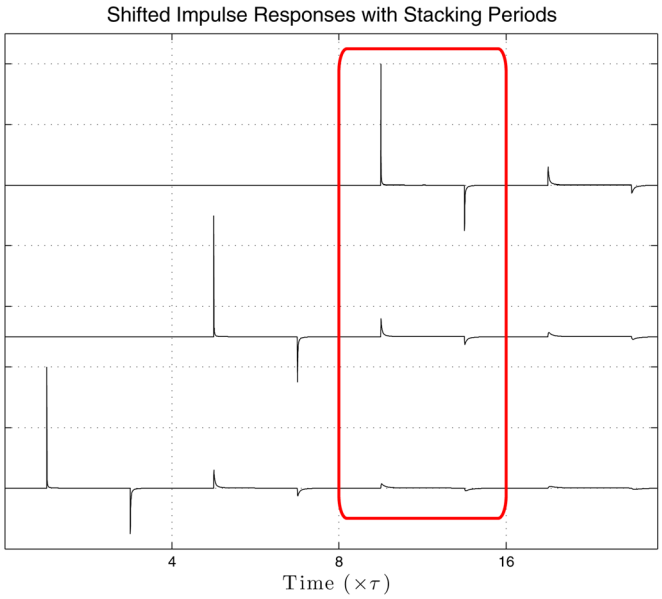

FIG. 10. (Color online) Reed instrument impulse responses are incrementally time shifted to the left by one period 4τ, the time taken for two round-trips from the mouthpiece to the bell and back again, showing a time alignment of the positive and negative pulses making up the current, and previous period(s).

which is exactly equivalent to Eq. (1), but more conveniently illustrates the makeup of the period of $4M$, where M is the time, in samples, needed to propagate the length of the bore. Equation (20) also lumps the losses into a single element $\eta(z)$, defined in Eq. (19), which is more easily estimated than the individual elements of which it is comprised.

In the presence of a periodic reed pulse, the instrument signal is also periodic, that is

$$\tilde{Y}_L(z) = \tilde{H}(z)\tilde{X}(z), \tag{21}$$

where the tilde represents the transforms of single periods of instrument and reed pulse signals, and where $\tilde{H}(z)$ is given by

$$\tilde{H}(z) = \left\{ z^{-M}\lambda(z)T(z)\left[\frac{1+z^{-2M}\eta(z)}{1-z^{-4M}\eta^2(z)}\right]\right\}_{4M}, \tag{22}$$

with the operator $\{\cdot\}_{4M}$ representing the transform of an impulse response made periodic, with period $4M$. Because the period is $4M$, instances of z^{-4M} can be removed and Eq. (22) may also be written as

$$\tilde{H}(z) = \left\{ z^{-M}\lambda(z)T(z)\left[\frac{1+z^{-2M}\eta(z)}{1-\eta^2(z)}\right]\right\}_{4M}. \tag{23}$$

Recall from the flow description in Sec. II that for every reed pulse, there are two round trips from the mouthpiece to the bell and back again, yielding a periodicity in the flow that corresponds to that of the pressure (as seen in Fig. 2), with the pressure showing two distinct halves—one where the pulse is positive and one where it is negative. With this in mind, it may be seen that the first term in the numerator of the periodic transfer function (23) contributes mostly to the first part of the period initiated by the positive pressure pulse, while the second term contributes mostly to the second half of the period, initiated by the negative pulse $2M$ later. That is, components of the output signal during the second half of the period have been roughly filtered by $\eta(z)$ compared to what they were in the first half of the period. Ideally, therefore, taking the spectral ratio of the first and second halves of the instrument period would yield an estimate of $\eta(z)$.

The difficulty is that in practice, the first and second parts of the clarinet period do not contain disjoint contributions. Though the time needed for the round-trip losses to decay is typically less than half a period, the duration of a reed pulse is ordinarily longer, causing an overlap in the contributions of the two phases of the period. This can be seen in Fig. 11, where an uncharacteristically narrow pulse yields distinct first and second halves of an instrument signal period, with one decaying completely before the onset of the next. The more realistic pulse width, however, produces a first and second half with no clear separation between the two. This smearing in time, and the difficulty in isolating the first and second parts of the period, make taking the spectral ratio directly an insufficient method for estimating $\eta(z)$.

In Ref. 16 an attempt was made to separate the time-aliased components by first considering their sum and their difference, effectively creating an artificial "echo" that cancels a portion of the feedback. In this solution, the spectral ratio of the sum and difference was used to develop an expression for the estimator $\eta(z)$. Though the period of the clarinet signal could be determined using pitch detection, and the half periods found at zero crossings, the cancellation echo was not sufficient for isolating the half periods. In addition, it was unclear where the period of the signal began.

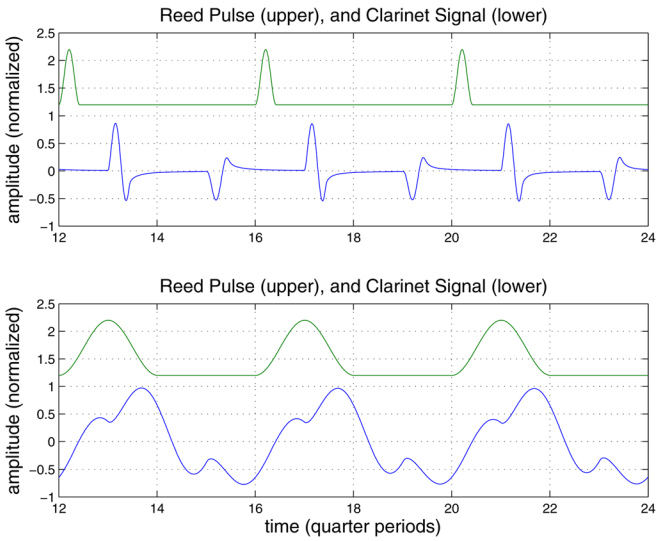

FIG. 11. (Color online) The first and second parts of a clarinet signal period are clear when the reed pulse width is significantly less than half the period (upper). More typically, however, the width approaches the half period, and as a result the clarinet signal will no longer contain disjoint contributions. This time aliasing makes it difficult to take the spectral ratios of the first and second halves of the period to obtain the estimate $\eta(z)$ in Eq. (19).

As $\eta(z)$ represents an attenuation, it is expected that the spectral ratio of the first and second halves of the period would be small, and thus another approach would be to find the point in time where the spectral ratio is minimized. This approach was found to be much less robust, however, than the preferred method of using the instrument signal autocorrelation computed over a sliding window.

B. Finding $\eta(z)$ using the autocorrelation method

The autocorrelation is zero phase by construction and thus naturally provides the beginning of the period. It also has clear first and second phases akin to what is seen in the clarinet signal period. The time evolution of the autocorrelation of a clarinet signal is shown in Fig. 12 by overlaying periods of a running autocorrelation computed at several times during the note. There is a dominant main lobe corresponding to the reed pulse, and an inverted secondary lobe corresponding to the reed pulse round trip along the instrument, with this structure becoming increasingly prominent as the note moves into the steady state.

These features may be explained by considering the power spectrum, the transform of the autocorrelation. The power spectrum of the periodic instrument signal can be written as

$$\left|\tilde{Y}_L(z)\right|^2 = \left|\tilde{H}(z)\right|^2 \cdot \left|\tilde{X}(z)\right|^2, \tag{24}$$

where $\left|\tilde{H}(z)\right|^2$ is given by

$$\left|\tilde{H}(z)\right|^2 = \left\{ |\lambda(z)T(z)|^2 \frac{1+\eta(z)\eta^*(z)+z^{-2M}(\eta(z)+\eta^*(z))}{|1-\eta^2(z)|^2} \right\}_{4M}, \tag{25}$$

which uses the fact that a time advance of $2M$ is equivalent to a time delay of $2M$ in the presence of a periodic impulse response of $4M$. The two lobes of the autocorrelation are then seen to be associated with the autocorrelation of the reed pulse filtered by $1+\eta(z)\eta^*(z)$ for the main lobe, and filtered by $\eta(z)+\eta^*(z)$ for the side lobe at the half period $2M$ later.

If the reed pulse were sufficiently short, then $\eta(z)$ could be found by forming the spectral ratio of the first and second halves of the autocorrelation, $(\eta(z)+\eta^*(z))/(1+\eta(z)\eta^*(z))$, and then solving numerically to obtain an exact solution for $\eta(z)$. However, as previously discussed, the volume flow pulse is typically longer than half a period, causing a smearing in time between the two halves. Therefore, improved results are expected by finding $\eta(z)$ using an optimization.

Note that if the autocorrelation were filtered by

$$H_c(z) = 1+\eta(z)\eta^*(z) - z^{-2M}(\eta(z)+\eta^*(z)), \tag{26}$$

the resulting sequence would have transform

$$\begin{aligned} &\left|\tilde{Y}_L(z)\right|^2 \cdot H_c(z) \\ &= \left|\tilde{H}(z)\right|^2 \cdot H_c(z) \cdot \left|\tilde{X}(z)\right|^2 \\ &= \left\{ |\lambda(z)T(z)|^2 \frac{(1+\eta(z)\eta^*(z))^2 - (\eta(z)+\eta^*(z))^2}{|1-\eta^2(z)|^2} \right\}_{4M} \\ &\quad \times \left|\tilde{X}(z)\right|^2, \end{aligned} \tag{27}$$

producing a cancellation at lag $2M$ and thus the expectation of little energy around the half period. Accordingly, $\eta(z)$ is estimated as the filter that produces minimum energy near the half period of the autocorrelation filtered by Eq. (26).

This approach is used to estimate $\eta(z)$ for the same clarinet note used in Sec. IV C, and is shown in Fig. 13 along with the same filter constructed using the measured reflection $\hat{R}_B(\omega)$, theoretical wall loss λ, and scalar mouthpiece/reed reflection $R_M = 0.9$ described in Sec. IV C. That the estimated

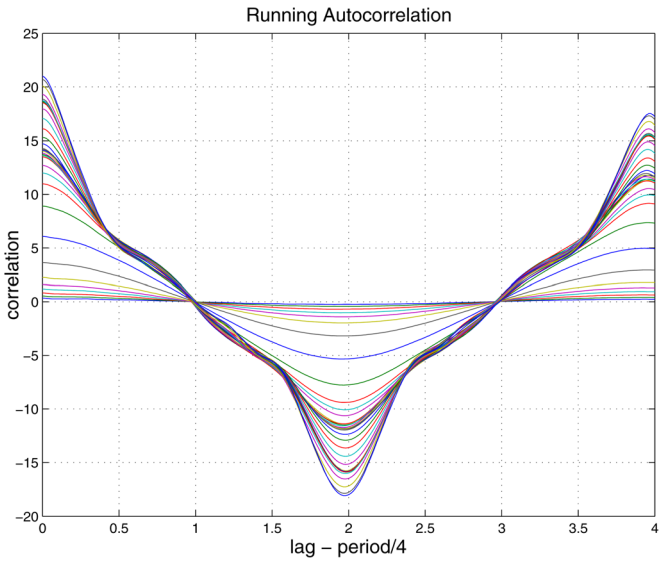

FIG. 12. (Color online) A running autocorrelation of a clarinet signal (overlaid) showing both the main positive lobe followed by the negative lobe, as well as the increased prominence of both as the clarinet tone modes into its steady state.

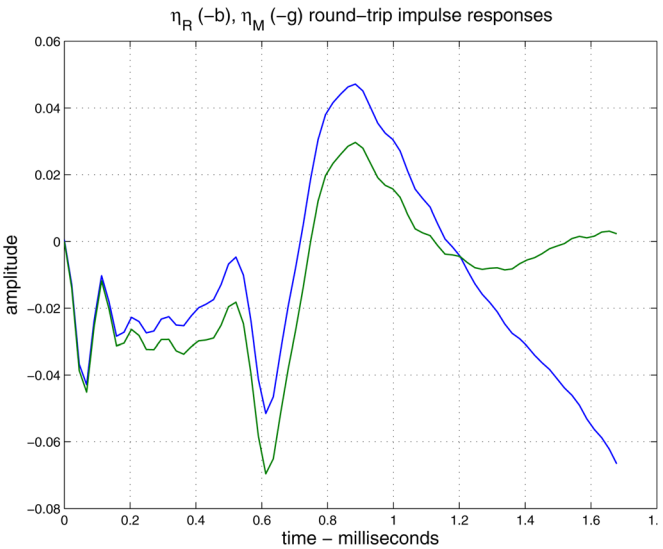

FIG. 13. (Color online) Round-trip losses η_M, constructed with theoretical λ, a scalar mouthpiece/reed reflection $R_M = 0.9$, and measured bell reflection $\hat{R}_B(\omega)$, and η_R, estimated as the filter that produces minimum energy near the half period of the running autocorrelation when filtered by Eq. (26).

and constructed filters η_R and η_M, respectively, shown in the time domain in Fig. 13 to better illustrate phase, are so similar in spite of being derived using very different techniques, gives confidence in the validity of the filter estimated from the recorded signal using the autocorrelation-optimization method.

The $\eta(z)$ estimated from the clarinet signal autocorrelation is then used to complete the inverse filter (3) which, when applied to the same clarinet note used in Sec. IV C, produces the reed pulse sequence shown in Fig. 14. The results are comparable, and even considerably improved, to those seen in Fig. 9, with the estimated reed pulses having the generally expected features—a slow rise and fall, followed by a short period of relatively small constant (or zero) flow. The fact that these features are even more prominent in Fig. 14 suggests an improvement to the preliminary results shown in Fig. 9, and possibly indicating that the unknown mouthpiece/reed reflection $R_M(z)$ has more significance than the simple scalar loss frequently used in many model approximations (including the one presented in Sec. IV).

Finally, it should be noted that though no assumption is made of the waveguide elements when estimating $\eta(z)$, the reed pulse sequence in Fig. 14 is obtained by completing the inverse filter (3) with the bell's measured transmission filter $\hat{T}_B(\omega)$, obtained as described in Sec. IV A. As previously noted, this is expected to change during performance and therefore its use presents an approximation. Since, however, it is not part of the recursive portion of the inverse filter, its approximation is expected to have less impact on the results, since an accurate $\eta(z)$, which represents recursive losses in the instrument, has considerably more importance. Dynamic estimation of the bell's transmission filter is left for future work. In the current application, however, as described in Sec. I, these results are sufficient for extracting and characterizing the reed pulse behavior for purpose of virtual instrument control.

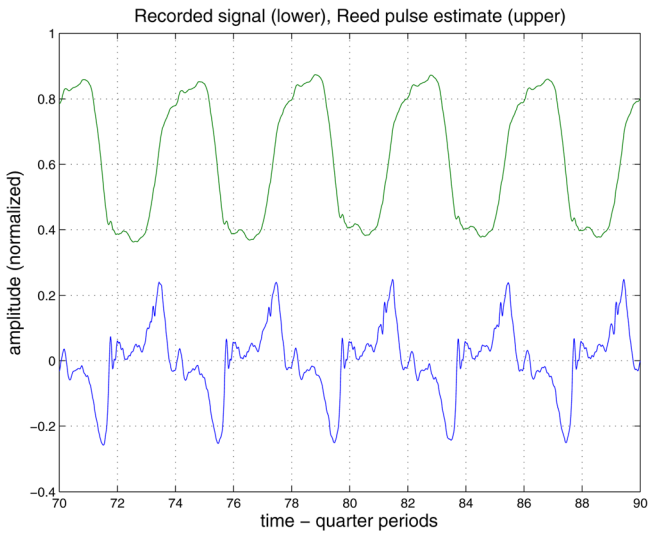

FIG. 14. (Color online) Reed pulse, estimated using the autocorrelation method and optimization (upper), along with original clarinet signal (lower). Notice improvements to the target in Fig. 9. This is likely due to the fact that the mouthpiece reflection is estimated as $R_M = 0.9$, but is actually included in the autocorrelation/optimization method for estimating η.

VI. CONCLUSION

In this work a method is presented for estimating the *reed pulse sequence* from a clarinet recording during instrument performance. An inverse filter is formed to obtain the volume flow given the clarinet signal recorded at the bell, but can be computed only by obtaining expressions for the bell reflection and transmission, reflection at the mouthpiece/reed, and the bore propagation losses. To obtain target behavior and a basis for evaluation, the special case of the clarinet's lowest note—played with all tone holes closed—is first considered. In this case, the inverse filter is constructed with the bell reflection and transmission filters estimated from measurement, the theoretical round-trip wall losses describing cylinders, and a simple scalar loss for the reed/mouthpiece reflection.

Subsequent results suggest that, when compared to the target, the time-varying component in the mouthpiece may be more significant than a scalar approximation. In addition, when the performer begins opening and closing tone holes during performance, the elements comprising the inverse filter become time varying, thus invalidating both the use of the bell reflection and transmission filters obtained *a priori* and the theoretically modeled wall loss filter for cylindrical tubes.

To address the time-varying nature of the estimation problem, the round-trip loss $\eta(z)$ in the bore, a filter lumping propagation and boundary loss, is estimated from the clarinet signal by first considering the signal's periodic structure, with the period having two distinct halves, one where the pulse is positive and one where it is negative. It is shown that this may be interpreted as components of the output signal during the second half of the period being roughly filtered by $\eta(z)$ compared to what they were in the first half of the period. Because of time-aliasing between the first and second halves, however, along with the difficulty in finding the beginning of the period, taking the spectral ratio of the first and second halves of the instrument period is insufficient for estimating $\eta(z)$.

The solution presented here for estimating the round-trip loss $\eta(z)$ and subsequent computation and application of the inverse filter involves taking the clarinet signal's running autocorrelation. As the autocorrelation preserves the periodicity and is zero phase by construction, it naturally provides the beginning of the period. The autocorrelation also displays a positive and negative lobe, the features of which are explained by considering the signal's power spectrum, the transform of the autocorrelation. The round-trip filter $\eta(z)$ is thus iteratively estimated by constructing an optimization function from the first and second phases of the autocorrelation, which, when applied to the autocorrelation of the periodic reed pulse, would cause a cancellation (or noticeable reduction in energy) at the half period for optimal $\eta(z)$. Thus $\eta(z)$ is iteratively estimated as the filter producing minimum energy near $2M$ for a periodic sequence with period $4M$.

The filter $\eta(z)$ is used to complete the inverse filter, which is then successfully applied to the clarinet signal to yield a sequence of reed pulses having the generally expected features of volume flow—a slow rise and fall, followed by a

period of constant (or zero) flow indicating a closed reed. As the reed pulse holds information related to embouchure and input pressure, its estimation can allow for further extracting of playing parameters by observing pulse characteristics such as contours, closure rates, value crossings. etc., or by calibrating to the output of a physical model of a reed, allowing for estimation of physical playing parameters such as blowing pressure or the reed tension/resonance.

ACKNOWLEDGMENTS

We would like to sincerely thank the Natural Sciences and Engineering Research Council of Canada (NSERC) for their support. Many thanks are also extended to the reviewers whose comments have greatly strengthened the quality of this work, and undoubtedly, its future development.

[1]M. Burtner, "The metasaxophone: Concept, implementation, and mapping strategies for a new computer music instrument," Organ. Sound **7**, 201–213 (2002).
[2]M. S. O'Modhrain, "Playing by feel: Incorporating haptic feedback into computer-based musical instruments," Ph.D. thesis, CCRMA, Stanford University, Stanford, CA, 2000.
[3]G. Scavone and A. da Silva, "Frequency content of breath pressure and implications for use in control," in *Proceedings of the International Conference on New Interfaces for Musical Expression*, Vancouver, Canada (2005), pp. 93–96.
[4]A. da Silva, M. M. Wanderley, and G. Scavone, "On the use of flute air jet as a musical control variable," in *Proceedings of the International Conference on New Interfaces for Musical Expression*, Vancouver, Canada (2005), pp. 105–108.
[5]D. Young, "A methodology for investigation of bowed string performance through measurement of violin bowing technique," Ph.D. thesis, Massachusetts Institute of Technology, Cambridge, MA, 2007.
[6]E. Guaus, J. Bonada, A. Perez, E. Maestre, and M. Blaauw, "Measuring the bow pressing force in a real violin performance," in *Proceedings of the International Symposium on Musical Acoustics (ISMA 07)*, Barcelona, Spain (2007).
[7]E. Maestre, "Data-driven statistical modeling of violin bowing gesture parameter contours," in *Proceedings of the International Computer Music Conference (ICMC 2009)*, Montreal, Canada (2009).
[8]T. Smyth, J. Abel, and J. O. Smith, "The estimation of birdsong control parameters using maximum likelihood and minimum action," in *Proceedings of the Stockholm Music Acoustics Conference (SMAC 03)*, Stockholm, Sweden (2003), pp. 413–416.
[9]S. Serafin and D. Young, "Bowed string physical model validation through use of a bow controller and examination of bow strokes," in *Proceedings of the Stockholm Music Acoustics Conference (SMAC-03)*, Stockholm, Sweden (2003), pp. 99–102.
[10]S. Serafin, J. O. Smith, and H. Thornburg, "A pattern recognition approach to invert a bowed string physical model," in *Proceedings of the International Symposium on Musical Acoustics (ISMA 2001)*, Perugia, Italy (2001), pp. 241–244.
[11]J. Makhoul, "Linear prediction: A tutorial review," Proc. IEEE **63**, 561–580 (1975).
[12]H.-L. Lu and J. O. Smith, "Joint estimation of vocal tract filter and glottal source wave-form via convex optimization," in *IEEE Workshop on Applications of Signal Processing to Audio and Acoustics (WASPAA'99)*, New Paltz, NY (1999), pp. 79–92.
[13]T. Helie, C. Vergez, J. Levine, and X. Rodet, "Inversion of a physical model of a trumpet," in *Proceedings of the 38th IEEE Conference on Decision and Control*, Phoenix, AZ (1999), Vol. 3, pp. 2593–2598.
[14]M. B. M. Sterling, X. Dong, and M. Bocko, "Representation of solo clarinet music by physical modeling synthesis," in *Proceedings of the IEEE International Conference on Acoustics Speech and Signal Processing (ICASSP 2008)*, Las Vegas, NV (2008), pp. 129–132.
[15]M. van Walstijn and G. de Sanctis, "Towards physics-based re-synthesis of woodwind tones," in *19th International Congress on Acoustics*, Madrid, Spain (2007).
[16]T. Smyth and J. Abel, "Estimating the reed pulse from clarinet recordings," in *Proceedings of the International Computer Music Conference (ICMC 2009)*, Montreal, Canada (2009), pp. 235–238.
[17]J. O. Smith, "Physical audio signal processing for virtual musical instruments and audio effects," http://ccrma.stanford.edu/~jos/pasp/(2008) (Last viewed June 20, 2011).
[18]V. Välimäki, J. Pakarinen, C. Erkut, and M. Karjalainen, "Discrete-time modelling of musical instruments," Rep. Prog. Phys. **69**, 1–78 (2006).
[19]T. Smyth and F. S. Scott, "Trombone synthesis by model and measurement," EURASIP J. Adv. Signal Process. **2011**, 151436 (2011), doi:10.1155/2011/151436.
[20]T. Smyth and J. Abel, "Estimating waveguide model elements from acoustic tube measurements," Acta Acust. Acust. **95**, 1093–1103 (2009).
[21]A. Farina, "Simultaneous measurement of impulse response and distortion with a swept-sine technique," in *Proceedings of the 108th AES Convention*, Paris, France (2000), pp. 18–22.
[22]T. Smyth, J. Abel, and J. O. Smith, "The feathered clarinet reed," in *Proceedings of the International Conference on Digital Audio Effects (DAFx'04)*, Naples, Italy (2004), pp. 95–100.
[23]N. H. Fletcher and T. D. Rossing, *The Physics of Musical Instruments* (Springer, New York, 1995), pp. 401–414.
[24]A. Hirschberg, R. van de Laar, J. Marrou-Maurières, A. Wijnands, H. J. Dane, S. G. Kruijswijk, and A. J. M. Houtsa, "A quasi-stationary model of air flow in the reed channel of single-reed woodwind instruments," Acustica **70**, 146–154 (1990).
[25]J.-P. Dalmont, J. Gilbert, and S. Oliver, "Nonlinear characteristics of single-reed instruments: Quasi-static volume flow and reed opening measurements," J. Acoust. Soc. Am. **114**, 2253–2262 (2003).
[26]J. Abel, T. Smyth, and J. O. Smith, "A simple, accurate wall loss filter for acoustic tubes," in *Proceedings of the International Conference on Digital Audio Effects(DAFX 2003)*, London, UK) (2003), pp. 53–57.
[27]www.opensoundcontrol.org (Last viewed April 24, 2012).